Proceedings of the Fifth IIEEJ International Workshop
on Image Electronics and Visual Computing 2017
Da Nang, Vietnam, February 28- March 3, 2017

RADIATION CHARACTERISTICS OF A SMALL NORMAL-MODE HELICAL ANTENNA FOR INTERNAL HUMAN BODY SENSING

Nguyen Thanh Tuan, Rasyidah Hanan binti Mohd Baharin, Yoshihide Yamada
Malaysia-Japan International Institute of Technology, Universiti Teknologi Malaysia
Kuala Lumpur, Malaysia

Dang Tien Dung, Nguyen Quoc Dinh
Department of Fundamentals of Radio and Electronics Engineering
Le Quy Don Technical University
Hanoi, Vietnam

Naobumi Michishita
Department of Electric and Electronics Engineering
National Defense Academy
Yokosuka, Japan

ABSTRACT

Recently, many types of radio sensors are being developed for human healthcare systems applications. A human sensing requires very small RF equipment (antenna and circuit). Antenna plays an important role in enhancing transmission efficiency as well as quality of diagnostic image. Normal-Mode Helical Antenna (NMHA) is one of promising candidate because of its high transmission efficiency in very small size. For human body sensing applications, studies using an electromagnetic simulator were made. However, measurement in practical environment has not been made yet. In this paper, the situation of antenna inside a human body is achieved by putting the antenna in a human body phantom. Measured antenna input impedance and radiation patterns at frequency of 402 MHz are compared with simulation results. Through good agreements of measured and calculated results, transmission efficiency of NMHA as antenna in human body sensor is promising. The contribution of NMHA for improvement of diagnostic image will be expressed in next study.

Keywords— NMHA, human body sensing

1. INTRODUCTION

With the recent development of wireless sensing for human body, doctors are able to monitor the health of patients via implanted sensors during treatment or surgery. In implantable applications, antennas are required to be small in size but high radiation efficiency because transmission performance plays an important role in improving quality of diagnostic image. Some design antennas for Wireless Capsule Endoscopy (WCE) have been proposed such as spiral antenna [1], conformal chandelier meandered dipole antenna [2], outer-wall loop antenna [3] and conformal outer wall antenna [4]. However, our target is to design antenna for micro sensors of observing the inside of blood vessels. Normal-Mode Helical Antenna (NMHA) is one of the promising candidates, which can obtain high radiation efficiency at very small size in free space condition [5][6][7]. Human body can be considered as lossy material because it includes high permittivity and conductivity [8]. In the case of human body condition, electrical characteristics of NMHA should be studied.

In this paper, antenna performances of NMHA are investigated when implanted inside environment of human muscle. A simulation model is built on a commercial electromagnetic simulator FEKO 7.0 [9] and solved by computational electromagnetics of Method of Moment (MoM). A self-resonant structure from simulated results will be selected to do experiments with artificial human phantom that consists of electrical constants similar to that of practical human muscle. Antenna performances such as input impedance, antenna bandwidth and radiation patterns are obtained. From good efficiency of NMHA in practical human body, the quality of diagnostic image is promising to be improved.

2. SIMULATION MODEL

Simulation model of NMHA used in human muscle is simplified as shown in Fig. 1. NMHA is embedded inside a dielectric cylinder with dimensions of 60 x 60 mm as representation of human muscle. *H, D, N* indicates height, diameter of antenna and number of turns, respectively. A narrow air gap of 1 mm is put between antenna and material to avoid simulation errors. In practical biomedical application, the real human body is much more complicated with layers of tissue on top of another, with different permittivity, ε_r and conductivity, σ. It is important to note that the main purpose of the simplified model implemented in this paper is to study the fundamental characteristics of NMHA when implanted inside human body.

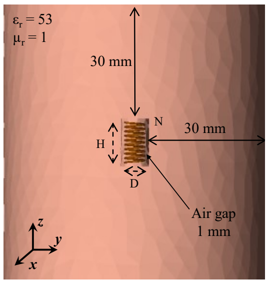

Fig. 1 Simulation model

Table. 1 Simulation parameters

Simulator	FEKO 7.0 (MoM)
Frequency	402 MHz
d	0.5 mm
Number of turns	N = 5; 7; 9
Metallic wire	Copper (σ = 58 x 10^6 [1/Ωm])
Dielectric constant of human muscle	ε_r= 53; μ_r = 1 σ_1 = 0.15 (S/m) ; σ_2= 0.89 (S/m) Mass density: 1040 (kg/m^3)
Mesh size of antenna wire	λ_g/100
Mesh size of material	λ_g/40

Simulation parameters of NMHA used in human muscle are shown in Table. 1. By using Method of Moment, surface of antenna wire and material will be divided into small meshes to calculate current distributions. Mesh size of antenna wire and material are set to be λ_g/100 and λ_g/40 with λ_g is wavelength in material. Metallic wire is defined as copper with conductivity σ = 58 x 10^6 [1/Ωm]. The actual dielectric constant of human muscle at 402MHz was clarified by Samii [8] where ε_r = 58.8 and conductivity, σ = 0.84. However, for phantom fabrication, it is difficult to obtain the exact value. Thus, our simulation parameter is adjusted based on the ε_r and σ of the fabricated phantom, which is ε_r= 53; relative permeability μ_r= 1 and conductivity σ_2 = 0.89 (S/m). However, low conductivity phantom with σ_1 = 0.15 (S/m) is also applied to estimate power absorption by human body.

By adjustment of *H* and *D*, self-resonant structures of various *N* are obtained in Fig. 2. Solid lines indicate structures for σ_2 = 0.89 (S/m), dotted lines indicate structures in case of σ_1 = 0.15 (S/m). Antenna diameter (*D*) becomes smaller with more number of turns (*N*) [10]. The difference in self-resonant structures are not significant in case of σ_2 = 0.89 (S/m) and σ_1 = 0.15 (S/m), therefore, conductivity can be considered not affecting self-resonance. Structure P in Fig. 2 is selected to do experiments.

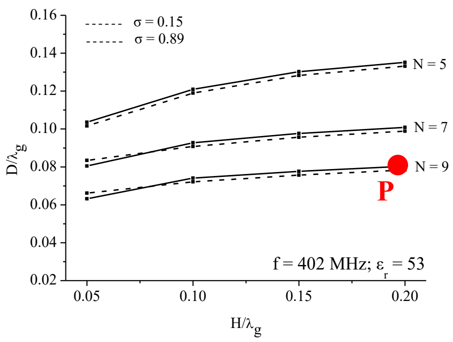

Fig. 2 Self-resonant structures

3. EXPERIMENT SETUP

Experimental setups are shown in Fig. 3. Antenna with dimension of *H* x *D* x *N*, 20 x 8.2 mm x 9 turns is put inside phantom with coordinate axes shown in Fig. 3(a). Typical characteristics of antenna such as input impedance and antenna bandwidth will be measured by Vector Network Analyzer (VNA) as shown in Fig. 3(b).

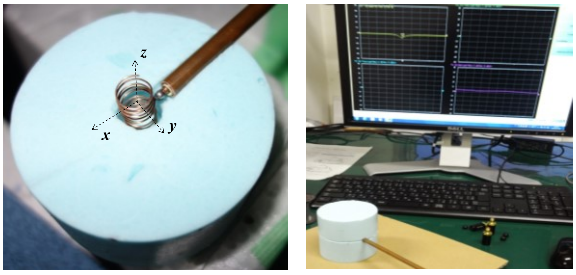

(a) NMHA in phantom (b) Input impedance measurement

Fig. 3 Experimental setup

Table. 2 Electrical parameters of phantom

Phantom 1	ε_r= 53; μ_r = 1; σ_1 = 0.15 (S/m)
Phantom 2	ε_r= 53; μ_r = 1; σ_2 = 0.89 (S/m)

In measurement, two kinds of phantom are utilized with electrical constants presented in Table. 2. Both phantoms have same relative permittivity ε_r= 53 but phantom 1 consists of low conductivity of σ_1 = 0.15 (S/m) and phantom 2 consists of higher conductivity of σ_2 = 0.89 (S/m). In both of these cases, input impedance and radiation patterns are measured to clarify antenna performances in human muscle condition.

4. MEASURED RESULTS

A. Input impedance

Antenna input impedance of NMHA in phantom 1 and phantom 2 are shown in Fig. 4 and Fig. 5, respectively. Because of antenna is resonant, so input impedance of NMHA equals to input resistance of NMHA.

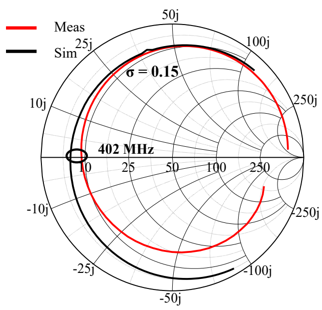

Fig. 4 Input impedance of NMHA in phantom

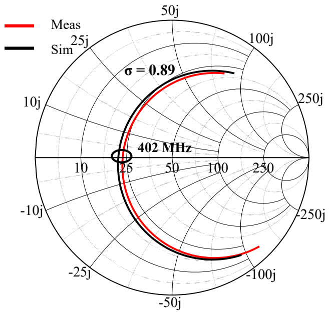

Fig. 5 Input impedance of NMHA in phantom 2

Input resistance of NMHA is expressed as the following:

$$R_{in} = R_{ant} + R_{abs} \quad (1)$$

Here, R_{in} indicates input resistance of NMHA in phantom; R_{ant} is resistance of antenna itself and R_{abs} is absorbing resistance by dielectric. Antenna resistance is presented as below:

$$R_{ant} = R_r + R_{ohm} \quad (2)$$

Here, R_r indicates radiated resistance; R_{ohm} indicates ohmic resistance of antenna wire. In both cases of phantom 1 and phantom 2, measured results and simulated results of input impedance agree well each other. However, input resistance of NMHA in phantom 1 is smaller than that of NMHA in phantom 2 with resistance of 9 Ω and 23 Ω, respectively. From simulation, antenna resistance of itself can be calculated of 0.8 Ω. Therefore, from Eq (1), absorbing resistances of phantom 1 and phantom 2 are calculated as $R_{abs(\sigma = 0.15)}$ = 7.2 (Ω) and $R_{abs(\sigma = 0.89)}$ = 22.2 (Ω), respectively. This concludes that dielectric loss mostly depends on conductivity of materials.

B. Antenna Bandwidth

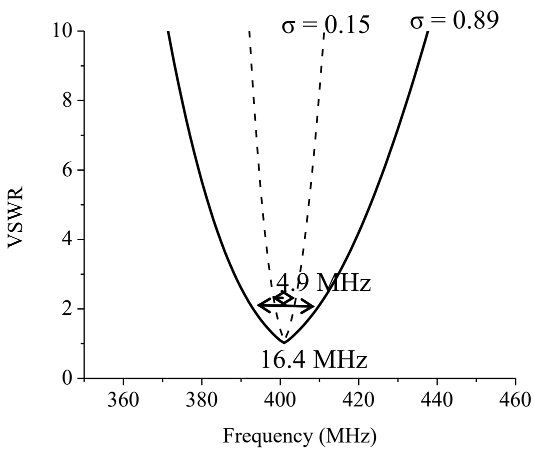

Fig. 6 Antenna bandwidth

Measured results of antenna bandwidth are shown in Fig. 6. At VSWR = 2, the bandwidth of NMHA in phantom 1 and phantom 2 are 4.9 MHz and 16.4 MHz, respectively. These correspond to fractional bandwidth of about 1.2% and 4.1%. It concludes that antenna bandwidth is wider in case of higher conductivity of human tissues. However, the antenna bandwidth of 4.1% is sufficient for data transmission of high resolution of diagnostic imaging from human sensing.

C. Radiation pattern

Radiation patterns of NMHA in phantom 1 (σ_1 = 0.15) in xy plane are shown in Fig. 7. Red line indicates measured results while black line indicates simulation results. Simulation and measurement have good agreement with omni-directional patterns. $E_{\theta max}$ and $E_{\varphi max}$ obtain about -31 dBi and -18 dBi, respectively. Radiation patterns of NMHA in phantom 1 in yz plane are shown in Fig. 8. Here, because of equivalent current model of NMHA consists of electric source from small dipole and magnetic source from small loop, radiation patterns of NMHA are similar to radiation patterns of dipole antenna or loop antenna. Simulation and measurement results agree well with each other. Practically, it is impossible to fabricate phantom with perfect dielectric constant of σ = 0 (S/m). However, from simulation results, antenna gain in case of σ = 0 is an approximation to the case of σ_1 = 0.15. With σ = 0, $E_{\theta max}$ and $E_{\varphi max}$ obtained are -30.5 dBi and -17.5 dBi, respectively.

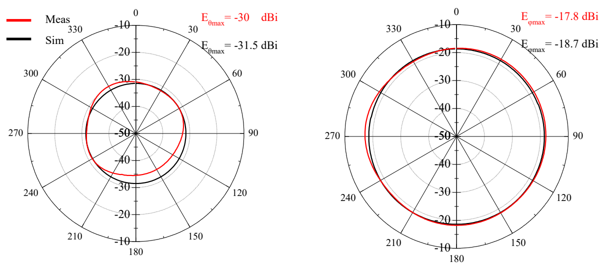

(a) E_θ (b) E_φ

Fig. 7 Radiation patterns of NMHA in phantom 1 (xy plane)

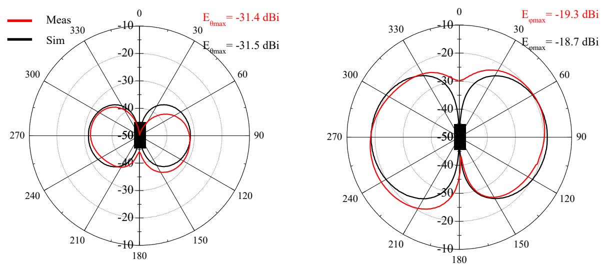

(a) E_θ (b) E_φ

Fig. 8 Radiation patterns of NMHA in phantom 1 (yz plane)

Similar to radiation pattern of NMHA in phantom 1, measured results of radiation patterns in case of phantom 2 (σ_2 = 0.89) in xy plane and yz plane are shown in Fig. 9 and Fig. 10, respectively. However, antenna gain becomes smaller than that of phantom 1 case and some distortion can be seen. It seems that phantom 2 absorbs more radiated power from antenna than phantom 1. Antenna gain of $E_{\theta max}$ and $E_{\varphi max}$ obtained are about -35 dBi and -24 dBi, respectively. It can be seen that antenna gain of NMHA in the case of phantom 2 is attenuated by effects of higher conductivity. Conductivity of phantom 2 (σ_2 = 0.89) is greater than conductivity of phantom 1 (σ_1 = 0.15), therefore, it can be concluded that conductivity of human tissues is the main factor which affects to antenna gain and antenna performance. Compare to antenna gain in case of σ = 0, antenna gain of $E_{\theta max}$ and $E_{\varphi max}$ is attenuated by about 4.5 dBi and 6.5 dBi due to the absorption caused by human muscle conductivity (σ_2 = 0.89).

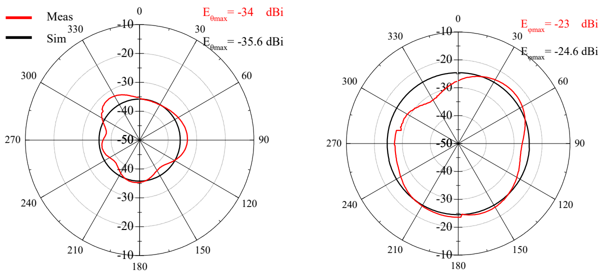

(a) E_θ (b) E_φ

Fig. 9 Radiation patterns of NMHA in phantom 2 (xy plane)

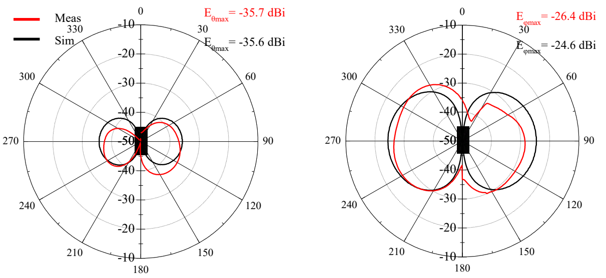

(a) E_θ (b) E_φ

Fig. 10 Radiation patterns of NMHA in phantom 2 (yz plane)

5. CONCLUSION

In order to estimate transmission efficiency of NMHA in human sensing application, a human body phantom is employed. Measured results of antenna input resistance is obtained as 9 Ω in case of σ_1 = 0.15 and 23 Ω in case of σ_2 = 0.89; antenna bandwidth achieves 4.1% in practical human muscle condition; and antenna gain obtain maximum -18 dBi in case of σ_1 = 0.15 and -24 dBi in case of σ_2 = 0.89. Compared to no loss condition of σ = 0, antenna gain is reduced by about 4.5 dBi to 6.5 dBi in human muscle condition. NMHA shows good performance and promising to meet the demand of enhancing the quality of diagnostic imaging. The improvement of image quality after applying high efficiency antenna will be presented in next study.

ACKNOWLEDGEMENT

Authors would like to give thanks to Prof. Masaharu Takahashi of Chiba University for his support in fabricating the phantom, and Prof. Hisashi Morishita of National Defense Academy for allowing us to use the anechoic chamber for measurement.

REFERENCES

[1]. S.I. Kwak, K. Chang and Y.J. Yoon, "Small spiral antenna for wideband capsule endoscope system," Electronics Letters, Vol. 42, Issue 23, pp. 1328 – 1329. November 2006.
[2]. P. Izdebski, H. RAjagopalan and Y. Rahmat-Samii, "Conformal ingestible capsule antenna: A novel Chandelier meandered Design", Special issue IEEE Trans. Antennas and Propag, Feb 209. pp.900 - 909.
[3]. S. Yun, K. Kim and S. Nam, "Outer wall loop antenna for ultra wideband capsule endoscope system", IEEE Antennas Wireless Propag. Lett. Vol. 9, pp. 1135 – 1138, Dec. 2010.
[4]. E. G. Lim, Z. Wang, F. Z. Yu, T. Tillo and K. L. Man, "Transmitter Antennas for Wireless Capsule Endoscopy", SoC Design Conference (ISOCC), 2012 International. Pp. 269 – 272.
[5]. Yoshihide Yamada and Naobumi Michishita, "Design Methods and Electrical Performances of Small Normal-Mode Helical Antennas," IEICE, Trans. Commun. B, vol. J96-B, no.9, pp.894-906, Sept. 2013.
[6]. W.G.Hong, W.H.Jung, Y.Yamada and N.Michishita, "High performance Normal Mode Helical Antenna for RFID Tags", IEEE International Sympo. on Aut. and Prop., pp.6023-6026, June 2007.
[7]. Quoc Dinh Nguyen, Naobumi Michishita, Yoshihide Yamada and Koji Nakatani, "Deterministic Equation for Self-Resonant Structures of Very Small Normal-Mode Helical Antennas", IEICE Trans.Commun., Vol.E94-B, No.5, PP.1276-1279, May 2011
[8]. J. Kim and Y. Rahmat-Samii, "Implanted Antennas inside a Human Body: Simulations, Designs and Characterizations," IEEE Trans. Microwave Theory & Tech., pp. 1934-1943, vol. 52, no. 8, Aug. 2004.
[9]. FEKO suite 7, EM Software & Systems
[10]. Nguyen Thanh Tuan, Yoshihide Yamada, Nguyen Quoc Dinh, Naobumi Michishita, "Self-Resonant Structures of Normal-Mode Helical Antennas embedded in Dielectric and Magnetic Materials", ATC, 627-632, ISSN 2162-1020, Oct 2015.